

# Automatic Camera Pose Determination from a Single Face Image

Li Wei<sup>†</sup>, Eung-Joo Lee<sup>\*\*</sup>, Soo-Yol Ok<sup>\*\*\*</sup>, Sung-Ho Bae<sup>\*\*\*\*</sup>, Suk-Hwan Lee<sup>\*\*\*\*\*</sup>,  
Young-Yeol Choo<sup>\*\*\*\*\*</sup>, and Ki-Ryong Kwon<sup>\*\*\*\*\*</sup>

## ABSTRACT

Camera pose information from 2D face image is very important for making virtual 3D face model synchronize with the real face. It is also very important for any other uses such as: human computer interface, 3D object estimation, automatic camera control etc. In this paper, we have presented a camera position determination algorithm from a single 2D face image using the relationship between mouth position information and face region boundary information. Our algorithm first corrects the color bias by a lighting compensation algorithm, then we nonlinearly transformed the image into  $YCbCr$  color space and use the visible chrominance feature of face in this color space to detect human face region. And then for face candidate, use the nearly reversed relationship information between  $C_b$  and  $C_r$  cluster of face feature to detect mouth position. And then we use the geometrical relationship between mouth position information and face region boundary information to determine rotation angles in both x-axis and y-axis of camera position and use the relationship between face region size information and Camera-Face distance information to determine the camera-face distance. Experimental results demonstrate the validity of our algorithm and the correct determination rate is accredited for applying it into practice.

**Keywords:** Face Detection, Mouth Detection, Color Space, Camera Position Determination

## 1. INTRODUCTION

During the past 30 years, many researchers have been working on determine camera position using 2D to 3D point or line correspondences. Such as: Perspective-n-Point (PnP) method [1] and Perspective-n-Line (PnL) method [2]. And there are a lot of researchers who work on these subjects: Ying & Jha[3] introduced a determine algorithm used information of parallel lines in a single 2D image, Bernas & Teisler[4] introduced an algorithm to determine the rotation angles in x-axis and y-axis of camera position in virtual studio. But almost all of these researches are aim at objects that contain correspond lines or points information. For human face, the camera position determination is also very important for dealing with the multiple pose, illumination and expression (MPIE) problem and face recognition in 3D face space.

[5] have introduced a synthetic exemplar based method for face recognition under different poses and lightings. So getting a human 3D face model is being possible. But use the individual's 3D face model to generate different PIE images for training the face recognition system is also a wasting time job, and on actual condition, the input face image is usually not the frontal face image. The camera may be on any place, the input face image may be captured from any angle. So on the actual condition, when these multiple position face images are inputted to the face recognition system, how to recognize these kinds of face image is still a problem to be researched[6].

In this paper, we will introduce an algorithm to detect the camera position from a single input face image which can be applied to 3D face space to set the view point. Through this method, we can make the virtual 3D face model synchronize to the real face at view point. For a single human face

image, there do not have any 3D point information or 3D line information. So using these information to detect the camera position is impossible. On the other ways, to detect the face region and mouth position can be much easier for an input human face image because their features are very strongly independent to others in image. So for a human face image, the relationship between mouth position and face region information can be employed to determine the camera position.

## 2. FACE REGION DETECTION ALGORITHM AND MOUTH POSITION DETECTION METHOD

In this section, an efficient and fully automatic framework is proposed for face region detection

\* Corresponding Author: Eung-Joo Lee, Address : (608-711) 535 YoungDang-Dong, Nam-Gu, Busan, Korea, TEL : +82-51-610-8372, FAX : +82-51-610-8846, E-mail : ejlee@tu.ac.kr

Receipt date : Apr. 30, 2007, Approval date : Dec. 10, 2007

\* Department of Information Communication Engineering, TongMyong University, Korea (E-mail : 12li-wei@163.com)

\*\* Department of Information Communication Engineering, TongMyong University, Korea (E-mail : ejlee@tu.ac.kr)

\*\*\* Department of Information Communication Engineering, TongMyong University, Korea (E-mail : sooyol@tu.ac.kr)

\*\*\*\* Department of Information Communication Engineering, TongMyong University, Korea (E-mail : shbae@tu.ac.kr)

\*\*\*\*\* Department of Information Communication Engineering, TongMyong University, Korea (E-mail : skylee@tu.ac.kr)

\*\*\*\*\* Department of Information Communication Engineering, TongMyong University, Korea (E-mail : yychoo@tu.ac.kr)

\*\*\*\*\* Department of Computer Engineering, PuKyung National University, Korea (E-mail : krkwon@pknu.ac.kr)

\* This research was supported by the MIC(Ministry of Information and Communication), Korea, under the U-Port ITRC(Information Technology Research Center) support program supervised by the IITA (Institute of Information Technology Assessment) (IITA-2007\_C1090-0701-0004).

and mouth position detection from an input single human face image. The framework consists of two parts: 1) Face region detection for face candidates and 2) mouth position detection in the detected face region image. The following subsections will describe these two parts in detail.

### 2.1 Face Region Detection

There are many kind of algorithm that used to detect the face region. R. Feraud[7], M. Pantic[8] discussed these algorithms. And [9] list a table to compare advantage and disadvantage of these face region detection algorithms. We will use the skin color information to detect human face because accuracy of the algorithm based on skin color information is better than others. The algorithm first estimates and corrects the color bias based on the lighting compensation technique which have been introduced in [10]. Fig. 1(a), (b) shows an input image and its' lighting compensation operating result.

The corrected red, green, and blue color components are then nonlinearly transformed into  $YCbCr$  color space and HSI color space. Fig. 2 shows these color spaces, respectively.

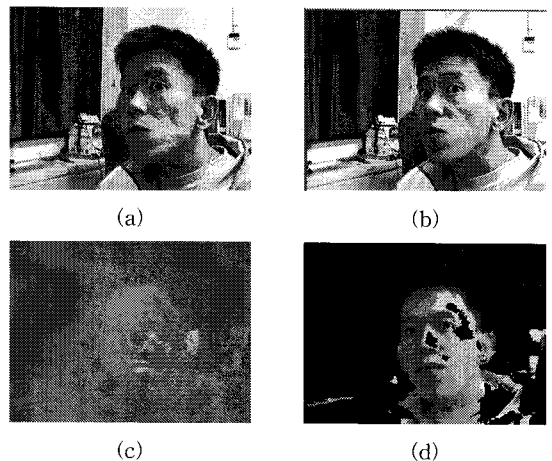


Fig. 1. Lighting Compensation and Face Detection Result: (a) Source Image, (b) Lighting Compensation Result Image, (c)  $C_r$  Image of Face and (d) Face Region Image.

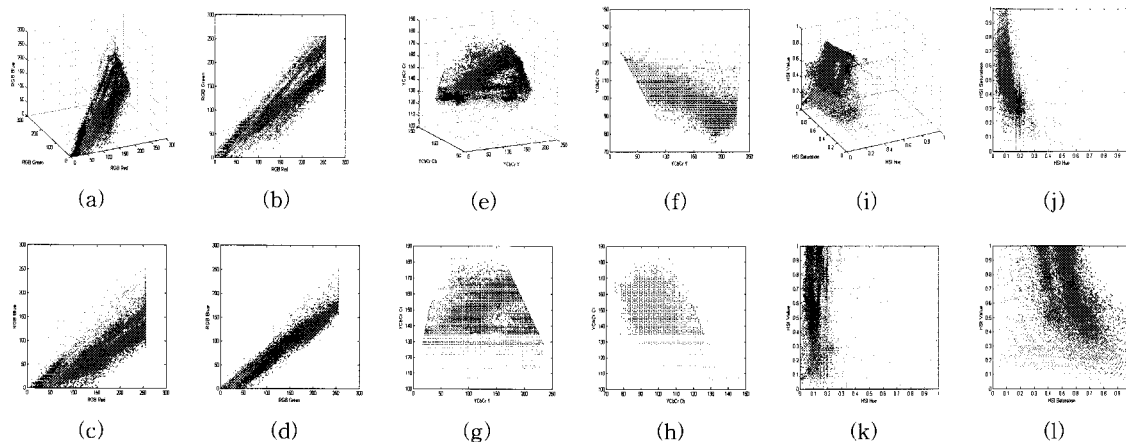


Fig. 2. The RGB, YCbCr and HSI Color Spaces of human face image shown in Fig. 1 (b) (blue dots represent the reproducible color on a monitor) and the skin tone model (red dots represent skin color samples, green dots represent mouth region color samples): (a) the RGB Space, (b) a 2D projection in the R-G subspace, (c) a 2D projection in the R-B subspace and (d) a 2D projection in the G-B subspace, (e) the YCbCr Space, (f) a 2D projection in the Y-C<sub>b</sub> subspace, and (g) a 2D projection in the Y-C<sub>r</sub> subspace, (h) a 2D projection in the C<sub>b</sub>-C<sub>r</sub> subspace, (i) the HSI Space, (j) a 2D projection in the H-S subspace, (k) a 2D projection in the H-I subspace and (l) a 2D projection in the S-I subspace.

Modeling skin color requires choosing an appropriate color space and identifying a cluster associated with skin color in this space. It has been observed that the normalized red-green (r-g) space [11] is not the best choice for face detection [12]. As shown in the above Fig. 2(e) (f) (g) (h), we can see that in the YCbCr color model, the C<sub>r</sub> values of face color are strongly independent of the background. Therefore, we can translate the input image from RGB color model to YCbCr color model, and the C<sub>r</sub> values can be employed to detect the region of face. According to our framework, we enactment that face region possess 70% of total region, so the histogram method can be employed to detect C<sub>r</sub> threshold of face, equations are shown as following:

$$S = \sum_{i=0}^{255} \text{Hist}(i), \quad CrTh = 70\% \times S \quad (1)$$

The detection result output image is shown in Fig. 1 (d).

## 2.2 Mouth Position Detection in Detected Face Region Image

Among the various facial features, eyes and mouth are the most prominent features for recognition and estimation of 3D head pose [13]. Most approaches for eye or mouth localization [14], H. Yan[15] are template-based. However, we directly locate mouth and face boundary based on their feature derived from both the luma and chroma of an image. The mouth and face features color information in multi-color models are shown in Fig. 2. Through comparing the mouth features in these color models, we can notice that in YCbCr color model, the C<sub>b</sub> and C<sub>r</sub> cluster of face have nearly reversed relationship, this relationship can also be noticed in C<sub>b</sub> image and C<sub>r</sub> image shown in Fig. 3(a) and Fig. 3(b), we can notice the relationship in details in C<sub>b</sub>-Y and C<sub>r</sub>-Y subspace, shown in Fig. 2(f) and Fig. 2(g), the color of mouth region contain stronger red component and weaker blue component than other facial region. Hence, the chrominance component C<sub>r</sub> is greater than C<sub>b</sub> in

the mouth region. We further notice that the mouth has a relatively low response in the  $C_b^2$  feature, but it has a high response in  $C_r^2$ . So in the mouth region the  $C_b^2$  and  $C_r^2$  will be closed and on other facial region they will be nearly reversed. Then we can make a multiply operation between  $C_b^2$  and  $C_r^2$ , so in the multiplied face image, mouth region contains stronger information than other face region. These operating equations are shown as following:

$$\text{MouthFeature} = \frac{\left(\frac{C_r^2}{\phi_1} \cdot \frac{C_b^2}{\phi_2}\right)}{\phi_3} = \frac{C_r^2 \cdot C_b^2}{\phi_1 \cdot \phi_2 \cdot \phi_3} \quad (2)$$

$$\phi_1 = 1.3 \cdot \frac{1}{M \cdot N} \sum_{(i,j) \in M,N} C_r, \quad \phi_2 = 1.3 \cdot \frac{1}{M \cdot N} \sum_{(i,j) \in M,N} C_b, \quad \phi_3 = 1.3 \cdot \frac{\phi_1 + \phi_2}{2} \quad (3)$$

Here both  $C_r^2$  and  $C_b^2$  are normalized to the range  $[0,255]$ , and  $M, N$  is width and height of face image. The parameter  $\phi_1$  is estimated as an average value of  $C_r$  and  $\phi_2$  is an average value of  $C_b$  and  $\phi_3$  is an average value of  $C_r$  and  $C_b$ . Fig. 3 (c), (d), (e) show the operating results for the image shown in Fig. 1.

And then we can use a pattern to detect the mouth region. Commonly mouth region possess  $1/5$  of total face region at least and  $2/3$  at most in horizontal direction and  $1/6$  at least and  $2/6$  at most in vertical direction, so here we select an average size between these size as a pattern, and use this pattern to detect the mouth region. Move the mouth pattern from left-top point to right-bottom point in Mouth Feature Image, and calculate sum value of all pixels in each pattern, and then select the

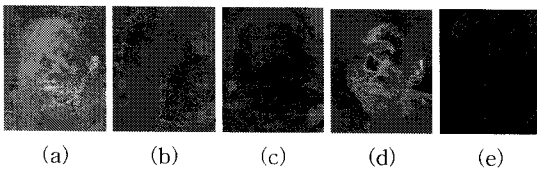


Fig. 3.  $C_r$ ,  $C_b$ ,  $C_r^2/\phi_1$ ,  $C_b^2/\phi_2$ , and Mouth Feature Image of Face: (a)  $C_r$  Image of Face, (b)  $C_b$  Image of Face, (c)  $C_r^2/\phi_1$  Image of Face, (d)  $C_b^2/\phi_2$  Image, and (e) Mouth Feature Image.

pattern whose sum value is maximal. Then we can confirm that the mouth region is contained in this pattern. Then we can calculate the center point position (also the mouth position) of this pattern. These operating equations are shown as following:

$$\text{Hist}(m,n) = \sum_{(m,n) \in M,N} \sum_{i=1}^{\frac{1}{14}M} \sum_{j=1}^{\frac{1}{6}N} \text{MouthFeature}(m+i, n+j),$$

$$\text{MaxValue} = \text{Max}(\text{Hist}(m,n))_{(m,n) \in M,N} \quad (4)$$

Fig. 4. shows the pattern operating result and Fig. 5 shows the mouth detection results.

### 3. CAMERA POSITION DETERMINATION ALGORITHM

As discussed in [16], the most important information of camera position is the rotation angles, any point (A) in 3D space can be rotated to new point (A') by the transformation matrices. So the most important job of camera position determination is to calculate the rotation angles ( $\alpha, \beta$ ) and the Camera-Face distance.

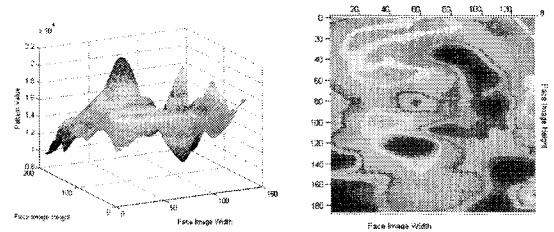


Fig. 4. Pattern Operating Results for Mouth Feature Image Shown in Fig 3(e): (a) 3D Diagram of Result, (b) Overlook of Depth Information for All Patterns (colors which changed from crimson to navy blue represent the depth information).

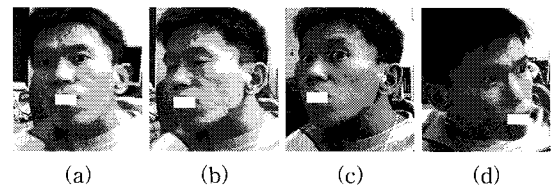


Fig. 5. Mouth Position Detect Result Outputs.

As shown in Fig. 5, we can easily find that, when camera rotated from one position to another (For Example: from frontal face to left 45 degree side in x direction), in the corresponding captured face image, the mouth position linearly moved from horizontal center to a corresponding position in the face region.

So here, we can use the linearly relationship information between mouth position and face region boundary to calculate the camera rotation angles ( $\alpha$ ,  $\beta$ ). And as we all know that when captured image from different distance, the size of face region is also different, as shown in Fig. 6 (d), they have linearly relationship, so we can use this relationship to determine the distance information. Firstly we make some definition about some Symbols used in our algorithm, and move the reference frame to the center point of face region, as the mouth and face region model shown in Fig. 6(a)

Here, M is symbol for mouth, FL for Face Left Boundary, FR for Face Right Boundary, FB for Face Bottom Boundary and FT for Face Top Boundary. The following subsections will describe the rotation angle determination algorithm for x-axis ( $\alpha$ ) and y-axis ( $\beta$ ) and Camera-Face distance information ( $D_{CF}$ ) in details.

### 3.1 Rotation Angle Determination for x-axis ( $\alpha$ )

Firstly, we point that  $\alpha=0$  in the frontal view

of face. And the range of  $\alpha$  is  $[-\pi/2, \pi/2]$  when face rotate from left side to right side. As shown in Fig. 6(b), the distance between mouth and face left boundary, mouth and face region right boundary can be calculated by

$$D_{ML} = |P_{Mouth}(x) - P_{FL}(x)| \quad D_{MR} = |P_{Mouth}(x) - P_{FR}(x)| \quad (5)$$

Here  $P_{Mouth}(x)$  is horizontal position mouth and  $P_{FL}(x)$  is horizontal position of face region left boundary and  $P_{FR}(x)$  is right boundary in the input image. Then we can gain horizontal setover between the two distances.

$$D_{HorSetover} = D_{ML} - D_{MR} \quad (6)$$

So we can set up a linearly equation to describe the relationship between  $\alpha$  and  $D_{HorSetover}$  as following:

$$\frac{D_{HorSetover}}{D_{LR}} = k \frac{\alpha}{\theta} + b \quad (7)$$

Here  $k$ ,  $\theta$  and  $b$  are constants.

We can calculate them by experiments in two special cases  $\alpha=0$  (Frontal View) and  $\alpha=\pi/2$  (Right Side View).

In case of Frontal View:  $\alpha=0$ ,  $P_{Mouth}(x)=0$  :  $D_{ML} = D_{LR} / 2$  and  $D_{MR} = D_{LR} / 2$ .

In case of Right Side View:  $\alpha=\pi/2$ ,  $P_{Mouth}(x) = D_{LR} / 2$  :  $D_{ML} = D_{LR}$  and  $D_{MR} = 0$ .

Then we can get an equation group from above equations as following:

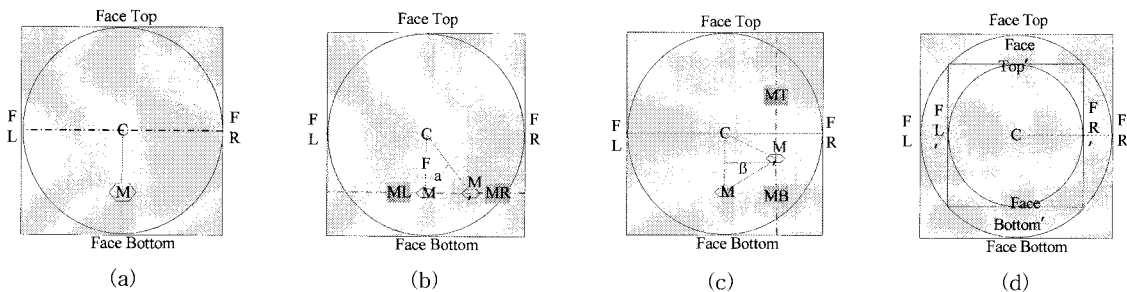


Fig. 6. Mouth and Face Region Model: (a) Common Frontal Side Model, (b)  $\alpha$  in Mouth and Face Region Model, (c)  $\beta$  in Mouth and Face Region Model and (d) Different Camera-Face Distance with Different Size of Face Region Model.

$$0 = \frac{(\frac{D_{LR}/2 - D_{LR}/2 - b) \times \theta}{D_{LR}} \textcircled{1}, \quad \frac{\pi}{2} = \frac{(\frac{D_{LR} - 0 - b) \times \theta}{D_{LR}} \textcircled{2}}{k} \quad (8)$$

And  $k$ ,  $\theta$  and  $b$  can be calculated from the equation group:  $b=0$ ,  $\theta=k \cdot (\pi/2)$ .

So the camera rotation angle for x-axis is:

$$\beta = \frac{\pi}{2} \times \frac{2P_{Mouth}(x) - D_{LR}}{D_{LR}} \quad (9)$$

Here  $D_{LR}$  and  $P_{Mouth}(x)$  can be easily gained from input 2D face image by using the Face Region and Mouth Position Detection algorithms discussed in section 2.

### 3.2 Rotation Angle Determination for y-axis ( $\beta$ )

And we also appoint that  $\beta=0$  in the frontal view of face. And the range of  $\beta$  is  $[-\pi/2, \pi/2]$  when face rotate from bottom side to top side. As shown in Fig. 6(c), the distance between mouth and face top boundary, mouth and face region bottom boundary can be calculated by

$$D_{MT} = |P_{Mouth}(y) - P_{FT}(y)| \quad D_{MB} = |P_{Mouth}(y) - P_{FB}(y)| \quad (10)$$

Here  $P_{FT}(x)$  is vertical position of face region top boundary in the input image. Then we can gain vertical setover between the two distances.

$$D_{VerSetover} = D_{MT} - D_{MB} \quad (11)$$

So we also can set up a linearly equation to describe the relationship between  $\beta$  and  $D_{VerSetover}$  as following:

$$\frac{D_{VerSetover}}{D_{TB}} = k \frac{\beta}{\theta} + b \quad (12)$$

Here  $k$ ,  $\theta$  and  $b$  are also constants for this equation.

Usually for the vertical direction, human mouth position is not in the center, so here we firstly move mouth position to the center in vertical direction

like this:  $P_{Mouth}'(y) = P_{Mouth}(y) - D_{MC}$ . So then we can use the similar equation as for x-axis, as the following:

$$\beta = \frac{\pi}{2} \times \frac{D_{VerSetover}}{D_{TB}} \quad (13)$$

And here:

$D_{VerSetover} = D_{MT} - D_{MB} = 2P_{Mouth}(y) - D_{TB} - 2D_{MC}$ , So the finally camera rotation angle for y-axis is:

$$\beta = \frac{\pi}{2} \times \frac{2P_{Mouth}(y) - D_{TB} - 2D_{MC}}{D_{TB}} \quad (14)$$

Here  $D_{TB}$  and  $P_{Mouth}(y)$  can also be easily gained from input 2D face image by using the Face Region and Mouth Position Detection algorithms discussed in section 2 and  $D_{MC}$  is an experience constant that can be gained from frontal view face image through many experiments. We have make many experiments on the FERET face database to confirm that commonly the value of  $D_{MC}$  is  $7/40$  of  $D_{TB}$ .

### 3.3 Camera-Face Distance Information Determination ( $D_{CF}$ )

As we all known than when an object close to the camera, size of this object in the captured image is larger than that from a far distance, and there is a linearly relationship between size information of object in image and Camera-Object distance information, which can be determined by using camera focus.

So for human face, we can set up a linearly equation to describe this relationship as the following:

$$\frac{S_{FR}}{S'_{FR}} = \frac{D_{CF}}{f} \Rightarrow D_{CF} = f \cdot \frac{S_{FR}}{S'_{FR}} \quad (15)$$

Here  $S_{FR}$  is actual size of face, and  $S'_{FR}$  is size of face region in captured image. Usually, for common use camera, focus of camera is not frequently changed, and for face,  $S_{FR}$  is also an experience constant, we can calculate an average face size as  $S_{FR}$  value through many experiments, so here we

can just use the  $S'_{FR}$  information which can be gained from the image by using the algorithm discussed in section 2 to determine the Camera-Face distance ( $D_{CF}$ ).

#### 4. EXPERIMENTAL RESULTS

We have evaluated our algorithm on several face image databases, including family photo collections. Most of the commonly used databases for face recognition, including the FERET face database contain frontal view gray-scale images only. So we must construct our database from MPEG7

videos, and USB camera for evaluating our algorithm. And we have evaluated our algorithm in different light conditions with different complex backgrounds and from different angle and distance.

Table 1 shows the results for only x-axis rotation from the same Camera-Face distance (human face only rotate from frontal side to left side or right side), Table 2 shows the results for only y-axis rotation from the same Camera-Face distance (human face only rotate from frontal side to top side or bottom side), Table 3 shows the results only for only Camera-Face distance and Table 4 shows the results for any other rotation in both

Table 1. Camera Position Determination Results for only x-axis Rotation




Face Image			
x-axis Rotation	2.7950°	13.3291°	40.2173°
y-axis Rotation	-3.6044°	- 2.3955°	- 4.9776°
Camera-Face Distance	0.4289 m	0.4629 m	0.4936 m

Table 2. Camera Position Determination Results for only y-axis Rotation




Face Image			
x-axis Rotation	5.5369°	- 3.0731°	3.7073°
y-axis Rotation	3.9477°	32.3358°	- 35.4263°
Camera-Face Distance	0.3407 m	0.3046	0.4013 m

Table 3. Camera Position Determination Results for only Camera-Face Distance







Face Image			
x-axis Rotation	41.9254°	39.0859°	34.7283°
y-axis Rotation	-17.3656°	-13.3982°	-15.8429°
Camera-Face Distance	0.4917 m	0.9766 m	2.2973 m

Table 4. Camera Position Determination Results for any Angle and Distance

Face Image			
x-axis Rotation	45.2795°	87.4596°	-38.3694°
y-axis Rotation	9.2014°	-5.1268°	12.3953°
Camera-Face Distance	0.4487 m	0.3815m	1.5309 m

x-axis and y-axis and from different distances. A Summary of the determination results (including the number of false determination, and accurate determination rate) on our self-build image database are presented in Tables 5, 6, 7 and 8 respectively. The database contains 30 peoples and for each people, there are 24 images that captured from different angle and different distance, each of size 320×240 pixels, and lighting conditions (including overhead lights and side lights) change from one image to another. A determined camera result is a *Correct Determination (CD)* if the

mouth position is found and camera rotation angle and Camera-Face distance are determined with a small amount of tolerance, otherwise it is called a *False Determination (FD)*. The determination rate is calculated by the ratio of number of correct determinations in a gallery to that of all human faces in the gallery. The *Correct Determination (CD)* Rate on our self-build database is more than 96% for all the poses when captured from frontal side, and when face rotate from frontal side to profile side, the determination rate will decrease, as shown in Table 5, in the second stage, the *Correct*

Table 5. Simulation Test Results of Camera Position for x-axis

Camera Rotation Angle	Test Images Number	CD Number	FD Number	Average Camera Angle	CD Rate (%)
( $\alpha=0, \beta=0$ )	30	29	1	$\alpha=0.0932^\circ \quad \beta=1.9179^\circ$	96.67
( $\alpha \approx 0, \beta \approx 0$ )	30	28	2	$\alpha=5.4472^\circ \quad \beta=4.7238^\circ$	93.33
( $\alpha \approx -\pi/4, \beta \approx 0$ )	30	28	2	$\alpha=-43.919^\circ \quad \beta=-3.8134^\circ$	93.33
( $\alpha \approx \pi/4, \beta \approx 0$ )	30	27	3	$\alpha=45.341^\circ \quad \beta=3.8283^\circ$	90
( $\alpha \approx -\pi/2, \beta \approx 0$ )	30	25	5	$\alpha=-86.459^\circ \quad \beta=-5.1268^\circ$	83.3
( $\alpha \approx \pi/2, \beta \approx 0$ )	30	26	4	$\alpha=88.2647^\circ \quad \beta=-14.977^\circ$	86.67

Table 6. Simulation Test Results of Camera Position for y-axis

Camera Rotation Angle	Test Images Number	CD Number	FD Number	Average Camera Angle	CD Rate (%)
( $\alpha=0, \beta=0$ )	30	30	0	$\alpha=0.1933^\circ \quad \beta=0.4568^\circ$	100
( $\alpha \approx 0, \beta \approx 0$ )	30	29	1	$\alpha=0.3532^\circ \quad \beta=2.4568^\circ$	96.67
( $\alpha \approx 0, \beta \approx -\pi/4$ )	30	28	2	$\alpha=5.7073^\circ \quad \beta=-45.425^\circ$	93.33
( $\alpha \approx 0, \beta \approx \pi/4$ )	30	28	2	$\alpha=-3.073^\circ \quad \beta=42.3358^\circ$	93.33
( $\alpha \approx 0, \beta \approx -\pi/3$ )	30	26	4	$\alpha=0.1043^\circ \quad \beta=-55.145^\circ$	86.67
( $\alpha \approx 0, \beta \approx \pi/3$ )	30	27	3	$\alpha=2.4523^\circ \quad \beta=63.545^\circ$	90

Table 7. Simulation Test Results of Camera Position for DCF

Camera Distance	Test Images Number	CD Number	FD Number	Average Camera Distance	CD Rate (%)
$D_{CF} = 1 \text{ m}$	30	30	0	0.9147 m	100
$D_{CF} = 1.5\text{m}$	30	29	1	1.4672 m	96.67
$D_{CF} = 2 \text{ m}$	30	28	2	2.0134 m	93.33
$D_{CF} = 2.5\text{m}$	30	29	1	2.5093 m	96.67
$D_{CF} = 3\text{m}$	30	28	2	3.0178 m	93.33
$D_{CF} = 4\text{m}$	30	27	3	3.9872 m	90



Table 8. Simulation Test Results of Camera Position for Any Angle and Distance:

Camera Position	Test Images Number	CD Number	FD Number	Average Camera Position ( $\alpha$ , $\beta$ , $D_{CF}$ )	CD Rate (%)
$\alpha \approx \pi/3$ , $\beta \approx -\pi/3$ , $D_{CF} = 1$ m	30	29	1	61.237°, -62.218°, 0.9752 m	96.67
$\alpha \approx \pi/5$ , $\beta \approx \pi/6$ , $D_{CF} = 2$ m	30	29	1	37.653°, 29.745°, 2.0342 m	96.67
$\alpha \approx \pi/2$ , $\beta \approx \pi/4$ , $D_{CF} = 1.4$ m	30	26	4	87.1245°, 45.535°, 1.4218 m	86.67
$\alpha \approx -\pi/4$ , $\beta \approx -\pi/10$ , $D_{CF} = 2.3$ m	30	27	3	-45.279°, -17.664°, 2.3130 m	90
$\alpha \approx -27\pi/100$ , $\beta \approx -2\pi/25$ , $D_{CF} = 1.6$ m	30	26	4	50.869°, -30.201°, 1.5174 m	86.67
$\alpha \approx -2\pi/25$ , $\beta \approx 3\pi/25$ , $D_{CF} = 3.2$ m	30	25	5	-16.211°, 12.783°, 3.1931 m	83.33

*Determination* rate decreases to 93.33%, and in the third stage, decreases to 86.67%, and for the profile face image, the rate is 83.3%. The reason for this is that when face rotates from frontal side to profile side, the left or right ear feature in  $Y-C_b$  subspace and  $Y-C_r$  subspace will become more similar to mouth feature. But mouth feature in these two subspaces will become more un conspicuous. So the *False Determination* Rate of mouth position detection will be higher, then the finally determination rate will be not very good when face rotates to profile side. And on the other ways, the experience constant value can also make errors for determining the rotation angle in y-axis and Camera-Face distance. But through many experiments, we can make the experiment constant more accurate to decrease the error.

## 5. CONCLUSIONS

We have presented a camera position determination algorithm for a single 2D face image using the relationship between mouth position information and face region boundary information. Our algorithm first corrects the color bias by a lighting compensation algorithm, then we nonlinearly transformed the image into  $Y C_b C_r$  color space and use the visible chrominance feature of face in this color space to detect human face region. And then for face candidate, use the nearly reversed relationship information between  $C_b$  and  $C_r$  cluster of face feature to detect mouth position.

And then we use the geometrical relationship between mouth position information and face region boundary information to determine rotation angles in both x-axis and y-axis of camera position and use the relationship between face region size information and Camera-Face distance information to determine the Camera-Face distance. The determination results on several image collections have been presented. Our object is to design a system use the camera position information to make the virtual 3D face model synchronize to the real world at view point, and for future work, we can capture a sample image from the virtual 3D face model, and use this sample image to compare with an input image from the real world captured at the same position, then we can make human face recognition with different PIE much more possible.

## REFERENCES

- [1] M.Fischler, R.Bolles, and Random, "Sample consensus: A Paradigm for Model Fitting with Application to Image Analysis and Automated Cartography," *ACM*, Vol.24, No.6, pp. 381-395, 1981.
- [2] H. Chen, "Pose Determination from Line-to-Plane Correspondences: Existence Solutions and Closed-form Solutions," *PAMI*, Vol.13, No.6, pp. 530-541, 1991.
- [3] Xianghua Ying and Hongbin Zha, "Camera Pose Determination From a Single View of Parallel Lines," *IEEE Transaction on ICIP*,

- Vol.3, pp. 1056-1059, 2005.
- [4] Martin Bernas and Martin Teisler, "Determination of the Camera Position in Virtual Studio," *IEEE International Symposium*, pp. 534-538, Dec. 2003
- [5] Charles. Beumier, "3D Face Recognition," *IEEE International Conference on Computational Intelligence for Homeland Security and Personal Safety Venice*, Italy, pp. 21-22, July 2004.
- [6] Mohamad Ivan Fanany and Itsua Kumazawa, "Analysis of Shape from Shading Algorithms for Fast and Realistic 3D face Reconstruction," *IEEE Trans. Circuits and Systems, APCCAS, Asia-Pacific Conference on*, Vol. 2, pp. 181-185, 2002.
- [7] R.Feraud, O.J.Bernier, J.-E. Viallet, and M. Collobert, "A Fast and Accurate Face Detection Based on Neural Network," *IEEE Trans. Pattern Analysis and Machine Intelligence*, Vol.23, No.1, pp. 42-53, Jan. 2001.
- [8] M. Pantic and L.J.M. Rothkrantz, "Automatic Analysis of Facial Expressions: The State of the Art," *IEEE Trans. Pattern Analysis and Machine Intelligence*, Vol.22, No.12, pp. 1424-1445, Dec. 1996.
- [9] Rein-Lien Hsu and Mohamed Abdel-Mottaleb, "Face Detection in Color Images," *IEEE Trans. Pattern Analysis and Machine Intelligence*, Vol.24, No.5, May 2002.
- [10] Xudong Xie and Kin-Man Lam, "An Efficient Illumination Compensation Scheme for Face Recognition," *IEEE Trans. 2004 8<sup>th</sup> International Conference on Control, Automation, Robotics and Vision*, Kunming, China, 6-9<sup>th</sup> December 2004.
- [11] L.M. Bergasa, M. Mazo, A. Gardel, M.A. Sotelo, and L. Boquete, "Unsupervised and Adaptive Gaussian Skin-Color Model," *Image and Vision Computing*, Vol.18, pp. 987-1003, Sep. 2001.
- [12] E. Saber and A.M. Tekalp, "Frontal-View Face Detection and Facial Feature Extraction Using Color, Shape and Symmetry Based Cost Functions," *Pattern Recognition Letters*, Vol.19, pp. 669-680, 1998.
- [13] A. Nikolaidis and I. Pitas, "Facial Feature Extraction and Determination of Pose," *Pattern Recognition*, Vol.33, pp. 1783-1791, 2000.
- [14] W. Huang, Q. Sun, C.-P. Lam, and J.-K. Wu, "A Robust Approach to Face and Eyes Detection from Images with Cluttered Background," *Int'l Conf. Pattern Recognition*, Vol.1, pp. 110-114, Aug. 1998.
- [15] K.M. Lam and H. Yan, "Locating and Extracting the Eye in Human Face Images," *Pattern Recognition*, Vol.29, No.5, pp. 771-779, 1996.
- [16] P.J. Phillips, H. Moon, S.A. Rizvi, and P.J.Rauss, "The FERET Evaluation Methodology for Face-Recognition Algorithm," *IEEE Trans. Pattern Analysis and Machine Intelligence*, Vol.22, No.10, pp. 1090-1104, Oct. 2000.



**Li Wei**

Received his B. S. in Dalian University of Light Industry in China (2002-2006), and now (2006-2008) his is a M. S. student of TongMyong University in Korea. His main research interests are in image processing computer vision Biometrics and face recognition.



**Eung-Joo Lee**

Received his B. S. , M. S. and Ph. D. in Electronic Engineering from Kyungpook National University, Korea, in 1990, 1992, and Aug. 1996, respectively. In March 1997, he joined the Department of Information Com-

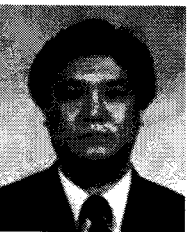
munication Engineering of Tongmyong University, Busan, Korea, as a professor. He has been worked as a Research Professor at Dalian Politech University in China from July 2005 to June 2006. His main research interests are in image processing, computer vision, and Biometrics. He has published many papers in the fields of Biometrics and participated in numerous government research projects.



**Soo-Yol Ok**

Received his M. S. and Ph. D. in Master's Program in sciences and Engineering, Doctoral Program in Engineering from Tsukuba University, Japan, in 1998, and July. 2001, respectively. In March 2004, he joined

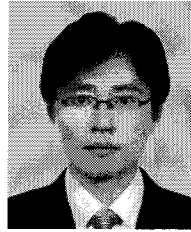
the Department of Game Engineering of Tongmyong University, Busan, Korea, as a professor. His main research interests are in Virtual Human Control, Game AI, and Computer Graphics.



**Sung-Ho Bae**

Received his B. S. , M. S. and Ph. D. in Electronic Engineering from Kyungpook National University, Korea, in 1991, 1993, and Aug. 1997, respectively. In September 1999, he joined the Department of Multimedia En-

gineering of Tongmyong University, Busan, Korea, as a professor. His main research interests are in digital watermarking, image processing, and computer vision.



**Suk-Hwan Lee**

He is a Professor of Tongmyong University in Korea. His main research interests are in Watermarking and Multimedia.



**Young-Yeol Choo**

received a B.S. and an M.S. degree in Control and Instrumentation Engineering from Seoul National University, Seoul, Korea in 1986 and 1988, respectively and a Ph. D. from the Pohang University of Science

and Technology, Pohang, Korea, in 2002. From 1988 to 2002, he has worked for posco as a senior researcher. At present, he is an Assistant Professor in the Dept. of Computer Engineering of Tongmyong University, Busan, Korea since 2002. He has been studied as a Visiting Scientist at Fraunhofer IESE (Institute of Experimental Software Engineering) from January 2005 to July 2005. He is Director of Ubiquitous Port ITRC supported by Ministry of Information and Communication of Korean Government from November 2006. His research interests include computer network, Ambient Intelligence, Ubiquitous Sensor Network, real-time systems and network security.



**Ki-Ryong Kwon**

received the B.S., M.S., and Ph. D. degrees in electronics engineering from Kyungpook National University in 1986, 1990, and 1994 respectively. He worked at Hyundai Motor Company from 1986-1988 and at Pusan Univer-

sity of Foreign Language from 1996-2006. In 2006, he joined the Pukyong National University, where he is an professor. His current research interests are in the area of digital image processing, multimedia security and watermarking, wavelet transform.